Characterisation of Reaction Waves in the Initiation of Detonation

Jeffrey Salmond and Nikos Nikiforakis

Laboratory for Scientific Computing
University of Cambridge, UK

Abstract. The ignition of condensed-phase explosives is investigated by simulating the reflection of a shock through nitromethane. The passage of the shock leads to the formation of a reaction wave. Of particular interest is the evolution of the reaction wave from when it emerges to when it eventually overtakes the precursor shock. We identify, locate and characterise transient, quasi-steady phenomena in the unsteady flow prior to the formation of a steady detonation wave. Results indicate that the reaction wave is composed of transient, quasi-steady waves similar to the ones observed in the gaseous case, albeit in a more complex combination.

Introduction

In this work we identify, locate and characterise reaction waves in the shock-induced ignition of the condensed-phase explosive nitromethane. We simulate an impact problem with the reflection of a precursor shock wave from a solid boundary in a semi-infinite, one-dimensional domain filled with explosive. Characterising and locating reaction waves in this idealised problem is an important first step to studying other ignition conditions, including hotspots.

The passage of a precursor shock through a combustible material may lead to the emergence of a reaction wave. Of particular interest is the evolution of the reaction wave from its emergence to when it eventually overtakes the precursor shock. This evolution is influenced by the strength of the precursor shock wave and the sensitivity of the explosive.

It has been observed (see, for example, Menikoff (2009), James & Lambourn (2006)) that the reaction wave in condensed-phase explosives may evolve to form a dome-like structure before overtaking the precursor shock wave and forming a detonation wave. Menikoff (2009) postulated that the dome-like structure is characteristic of heterogeneous explosives, such as PBXs. In contrast, a thermal runaway process leading to a detonation is characteristic of homogeneous explosives, such as liquid nitromethane [14]. While the sequence of events and the shape of the evolving waves has been discussed based on pressure (p,x) and density (ρ,x) spatial distributions and particle velocity histories, the nature of the evolving combustion-driven waves is unclear.

When a steady detonation wave has emerged and is mapped onto (p,v) (pressure versus specific volume) space it is easy to identify the steady-state structure by means of the CJ values and the von Neumann peak. However, when the flow field is transient and the waves have compound structure, an analysis based on spatial distribution has limitations. The emerging waves are characterised in the literature by terms such as "superdetonation", which are useful but are nevertheless incompatible with the standard textbook terminology of fundamental combustion waves based on the steady (p,v) diagram. Given the inherently transient nature of the evolving flow, a (p,v) space mapping, as in the steady detonation case, is not immediately obvious.

It is thus useful to revisit previous work by Clarke and co-workers in the context of the evolution of

1

gaseous detonations. The seminal work by Clarke (1989) established a theoretical foundation for the identification of transient, quasi-steady phenomena including weak detonations and fast flames, which appear as straight lines of negative slope on (p,v) space.

Singh and Clarke (1992) considered shock-induced ignition of a combustible gaseous mixture using a (p,v) space analysis to reveal that the evolving reaction wave was in fact composed of these quasi-steady waves which propagated in space as compound waves. Later, Nikiforakis and Clarke (1996) tracked these waves in two-dimensional space in the context of hotspot ignition in a gaseous mixture. This work illustrated that events that happen on the scale of bulk reaction can be found in the same form on the microscale of resolved hotspots.

More recently, Bates (2005) tracked these quasi-steady waves on (x,t) space and showed they can still be identified if the simple Arrhenius-based reaction rate law is replaced by a detailed chemistry model. This detailed chemistry model was also applied to a hydrogen-oxygen mixture at different levels of dilution by argon.

Some authors investigating condensed-phase explosives mapped their results onto (p,v) space. For example, Sharpe & Short (2004) presented simulations of a solid explosive modelled with the ideal gas equation of state and Handley (2010) performed simulations of HMX based PBXs with realistic equations of state and heterogeneous structure. In both of these works the evolution of the flow was plotted on (p,v) space. However, the analysis did not go as far as tracking quasi-steady waves.

It is the purpose of this work to apply the methodology described above to condensed-phase explosives and to identify transient, quasi-steady waves similar to the ones identified in the gaseous case. Although the characterisation of the evolving reaction waves is an interesting study in its own right, it is even more important to apply the same methodology to resolved simulations of hotspot ignition, as in the work by Nikiforakis & Clarke (1996). Understanding the reaction-generated flow due to hotspots by characterising the transient waves emanating in their vicinity, and their propagation into the bulk of the explosive, is key to the development of mesoscale models for shock initiation of heterogeneous explosives. The future development of these mesoscale models is the motivation for this work.

We consider liquid nitromethane as the working material as it has been extensively studied by analytical, numerical and experimental means so there is a wealth of data for validation purposes. Once its ignition behaviour is assessed as a neat substance, its heterogeneous state can be studied by artificially seeding it with impurities such as gas cavities and solid particles.

In the following sections we present the governing equations of flow and the necessary closure conditions, as well as a brief overview of the numerical methodology used to calculate their solution. The model is validated for steady-state detonation and shock-induced ignition against analytical, experimental and previously published numerical results. Finally, we present early and late stages of the evolving flow on (p,v) space and the complete wave structures on (x,t) space. Results indicate that the reaction wave emerging following the passage of a precursor shock is composed of transient, quasi-steady waves similar to the ones observed in the gaseous case, albeit in a more complex combination.

Governing Equations

In this work, we model the nitromethane system using the one-dimensional Euler equations augmented by an additional equation to evolve the mass fraction of the reactant. The two phases (reactant and product) are described by two distinct equations of state in Mie-Grüneisen form. The rate of reaction is modelled by a single-step Arrhenius expression.

In one space dimension, the system can be expressed in conservation form as

$$\frac{\partial}{\partial t}\mathbf{Q} + \frac{\partial}{\partial x}\mathbf{F}(\mathbf{Q}) = \mathbf{S}(\mathbf{Q}),$$

where the vector of conserved quantities $\mathbf{Q}$, the flux function $\mathbf{F}(\mathbf{Q})$ and the source term $\mathbf{S}(\mathbf{Q})$ are given by

$$\mathbf{Q} = \begin{pmatrix} \rho \\ \rho u \\ E \\ \rho \lambda \end{pmatrix}, \quad \mathbf{F}(\mathbf{Q}) = \begin{pmatrix} \rho u \\ \rho u^2 + p \\ u(E + p) \\ \rho u \lambda \end{pmatrix}, \quad \mathbf{S}(\mathbf{Q}) = \begin{pmatrix} 0 \\ 0 \\ 0 \\ \rho \mathcal{K} \end{pmatrix}.$$

The following notation is used: density ρ, specific volume v, velocity u, pressure p, total energy E, mass fraction λ and the rate law (to be defined later) as $\mathcal{K}$. The total energy E is defined as the sum of internal and kinetic energies,

$$E = \rho \left(e + \frac{1}{2} u^2 \right),$$

where e is the specific internal energy of the mixture. The mixture equation of state $e = e(v, p, \lambda)$ is calculated from two distinct equations of state for the reactant and product. Both component equations of state are in the generic Mie-Grüneisen form,

$$p(v, e) = p_{\text{ref}}(v) + \frac{\Gamma(v)}{v} \left(e - e_{\text{ref}}(v) \right),$$
$$e(v, p) = e_{\text{ref}}(v) + \frac{v}{\Gamma(v)} \left(p - p_{\text{ref}}(v) \right),$$

where $\Gamma(v)$ and the reference curves $p_{\text{ref}}(v)$ and $e_{\text{ref}}(v)$ are defined below.

The temperature of each material is calculated by

$$T(v, e) = T_0 + \frac{e}{c_v},$$

where T_0 is a reference temperature and the heat capacity c_v of the material is assumed to be constant. In the context of this work, this assumption reproduces experimental and theoretical values. The validity of this assumption will be explored in future work.

Mixture Equation of State

The mixture equation of state is defined by the two equations of state for the reactant and product, denoted with subscripts r and p respectively.

$$e_r = e_r(v_r, p_r), \quad e_p = e_p(v_p, p_p).$$

For this study, e_r is a linear Grüneisen equation and e_p is a pseudo-polytropic equation.

The mixture specific volume v is defined as a weighted sum of the two phase volumes v_r and v_p with the specific internal energy e as a similar weighted sum of the two specific internal energies e_r and e_p,

$$v = v_r (1 - \lambda) + v_p \lambda, \quad e = e_r (1 - \lambda) + e_p \lambda.$$

To close the system, assumptions must be made about the mixture. In this work, we make the commonly used assumption that the phases are in mechanical equilibrium (that is, equal velocities $u = u_r = u_p$ and pressures $p = p_r = p_p$). Furthermore, we assume that the two phases are in temperature equilibrium ($T_r = T_p$).

The assumptions of mechanical and temperature equilibrium have been examined by a variety of authors, including [2], [10] and [18], who have concluded that for most cases mechanical equilibrium occurs on very short timescales and non-equilibrium effects can be safely neglected. The evidence for temperature equilibrium is less well established, but in practice it gives reasonable results; Byers-Brown [4] and Stewart [23] have found that very similar solutions for the structure of the detonation wave can be obtained with either temperature equilibrium or thermal isolation. In future work we will explore the effect of this assumption.

To evaluate the mixture equation of state, we follow [23] and define an auxiliary parameter ϕ as the ratio of the phase specific volumes, $\phi = v_r / v_p$. This gives the partial volumes as

$$v_r(\phi) = \frac{\phi v}{\lambda + (1 - \lambda)\phi}, \quad v_p(\phi) = \frac{v}{\lambda + (1 - \lambda)\phi}.$$

Therefore, ϕ can be found as the solution of

$$f(\phi) = T_r \left(v_r(\phi), p \right) - T_p \left(v_p(\phi), p \right) = 0.$$

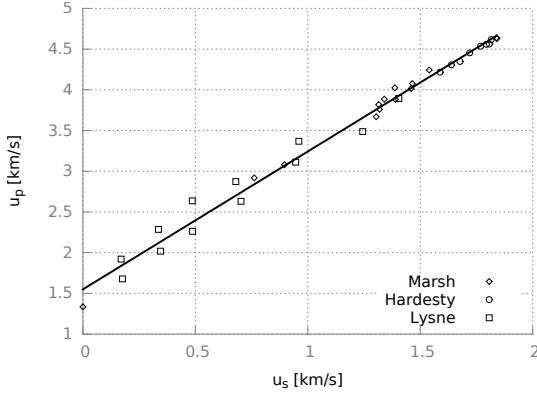This is solved using a numerical root finding technique.

3

Figure 1: Shock u_s and particle u_p velocity loci for liquid nitromethane. Experimental points are taken from [8], [11], [12] and [13]. The line is calculated from the linear Grüneisen equation of state with parameters from table 1.

Reactant Equation of State: Linear Grüneisen

We use the linear Grüneisen equation of state for the unreacted liquid nitromethane. This equation of state assumes that there is a linear relationship between the shock and particle velocities

$$u_s = a + bu_p,$$

where a and b are constants. The reference curves are derived from the $u_s - u_p$ relationship and are defined as

$$p_{ref}(v) = \frac{a^2 (v_0 - v)}{(v_0 - b(v_0 - v))^2},$$

$$e_{ref}(v) = \frac{1}{2}p_{ref}(v)(v_0 - v) - e_0,$$

and $\Gamma(v) = \Gamma_0$. The parameters used in this work are fitted to experimental data in [8], [11], [12] and [13]. The experimental (u_s, u_p) points and the fit are plotted in figure 1. The values are given in table 1.

Product Equation of State: Pseudo-Polytropic

We take a pseudo-polytropic equation of state for the gaseous products of the reactions and we choose

ρ_0 [kg/m^3]	1137
Γ_0	1
a [m/s]	1550
b	1.69
e_0 [J/kg]	0
T_0 [K]	300
c_v [J/kgK]	2185

Table 1: Parameters for the reactant equation of state. These values have been fitted to the experimental results in [8], [11], [12] and [13].

to define Γ as a rational polynomial,

$$\Gamma(v) = \frac{a_0 + a_1 v/v_0}{b_0 + b_1 v/v_0}.$$

The Mie-Grüneisen reference curves are defined as $p_{ref}(v) = 0$ and $e_{ref}(v) = -e_0$, and the values of the parameters are given in table 2. The values of these parameters were determined by fitting to isentrope data from an ideal detonation code [3].

ρ_0 [kg/m^3]	3781
a_0	5.59
a_1	0.51
b_0	0.45
b_1	2.60
e_0 [MJ/kg]	6.64
T_0 [K]	2680
c_v [J/kgK]	1142

Table 2: Parameters for product equation of state. These values were determined by fitting to isentrope data from an ideal detonation code [3].

Reaction Rate

For this work we use a first-order Arrhenius type reaction rate of the form:

$$\mathcal{K}(T) = A(1 - \lambda)\exp(-\mathcal{E}/T).$$

Other studies have used more complex rate expressions (for example, Menikoff [15] suggests a second-

4

order Arrhenius law and Tarver [24] suggests a pressure-based ignition and growth formulation). For the set of experiments conducted in this work, we have found that the simple first-order rate law gives reasonable results. This is illustrated in the validation section.

A range of studies (see for example [15], [19] and [24]) have found that values for the activation energy around $\mathcal{E} = 12.5 \times 10^3$ K give reasonable results. In this work, this value was varied slightly to $\mathcal{E} = 11.5 \times 10^3$ K, with $A = 2.6\,\text{ns}^{-1}$, in order to achieve a good match with experimental Pop plot data.

Numerical Methods

The final system of partial differential equations is solved by means of operator-splitting. The hyperbolic part is integrated by the weighted average flux (WAF) method [25], which is a second-order accurate Godunov-type finite volume method. The ordinary differential equation for the reactive source term is solved using a second-order Runge-Kutta scheme.

Validation

The validity of this model is assessed in the first instance by calculating the form of a steady state detonation. The Hugoniot locus and overdriven detonation locus (or Crussard curve) are shown in figures 2 and 3, and the von Neumann and Chapman-Jouget states are marked on each plot. The Hugoniot loci calculated from this material model demonstrate a good fit to the experimental data points. Figure 3 also includes a curve calculated from the theoretical work in [27] and again, good agreement is shown.

The pressure, specific volume and temperature at the key points on these plots are given in table 3, and these values are within the spread of values found in the literature (see [15] and [16] and references therein).

We can also assess the suitability of the model for shock initiation by comparing to experimental Pop plot data. Figure 4 shows experimental and simulation results for the time to ignition at different shock input
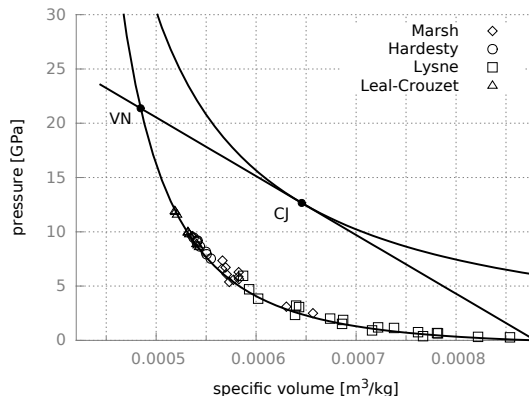

Figure 2: Nitromethane Hugoniot locus (lower curve) and overdriven detonation locus (upper curve). The von Neumann and Chapman-Jouget states are marked VN and CJ and are joined by a Rayleigh Line. Also shown are experimental points from Marsh [13], Hardesty [8], Lysne [12] and Leal-Crouzet [11].
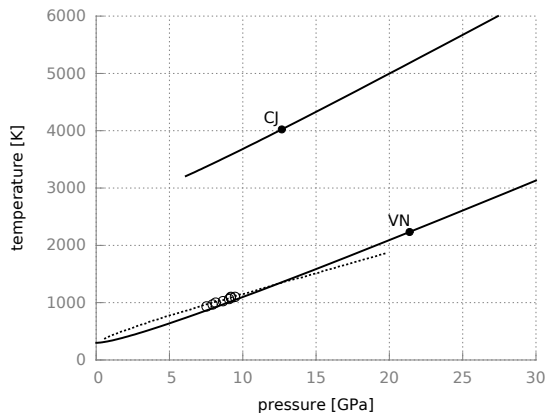

Figure 3: Nitromethane temperatures along the Hugoniot locus for reactants (lower curve) and products (upper curve) shown as a function of pressure. Also shown are experimental points from [8], and a curve (dashed line) calculated from the theoretical work in [27].

5

	v [m^3/kg]	p [GPa]	T [K]
Initial State	0.879×10^{-3}	10^{-4}	300
VN Spike	0.484×10^{-3}	21.4	2233
CJ State	0.645×10^{-3}	12.7	4023

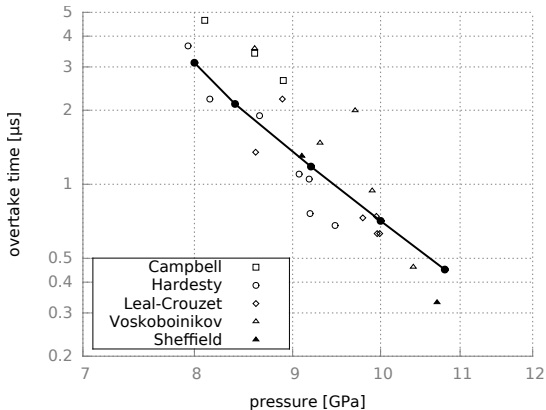Table 3: Initial, VN and CJ states for a steady detonation wave at 6.25 km s^{-1}.

Figure 4: Time to ignition as a function of input shock pressure. The line shows results from five numerical simulations using the material model described and points are from experiments in Campbell [5], Hardesty [8], Leal-Crouziet [11], Voskoboinikov [26] and Sheffield [adapted from [15]].

pressures. There is a large scatter in the experimental data, partly due to varying experimental techniques and definitions for ignition. A similar picture emerged when we varied the definition of ignition as a percentage of the amount of fuel consumed. Irrespective of the latter, the simulation results were within the spread of the experimental data but the curve shifted within that range. For clarity those measurements are omitted and we plot the time of the extreme case when the reaction wave is about to overtake the precursor shock.

Finally, we can assess the accuracy of the model and the simulation code by evolving a steady travelling detonation wave. Velocity histories from embedded gauges are shown in figure 5.

To confirm that the simulation attains the correct steady state, the numerical solution is overlaid on the reactant and product Hugoniots and Rayleigh line in figure 6. At the bottom right of the plot in figure 6, the initial state is at the lower crossing of the reactant Hugoniot and Rayleigh line. The shock compresses the fluid to the von Neumann spike at the upper crossing of the reactant Hugoniot and Rayleigh line. The two numerical points between the initial state and the von Neumann spike that lie close to the Hugoniot are artefacts of the numerical method which smears the shock over two computational cells. After the shock compression, the fluid reacts and expands along the Rayleigh line towards the CJ point. The final simulation point is at the CJ state where the Rayleigh line is a tangent to the product Hugoniot. Figure 6 shows that the simulation points lie, within numerical accuracy, on top of the Rayleigh line.

Numerical Results

To investigate the shock induced ignition of nitromethane, simulations designed to represent a gas gun experiment were performed. The setup of the experiment is represented with the explosive material initially moving at high speed into a stationary, reflective domain boundary. The reflective boundary is not an exact representation of the impactor, but it is suitable to recreate the important features of the experiment.

A time sequence of pressure and reaction progress profiles is shown in figure 7. A sustained shock of 9.2 GPa moves into the material from the left hand boundary eventually leading to a thermal runaway. A reaction wave moves into the temperature gradient generated by the passage of the precursor shock which steepens and eventually develops a discontinuity which finally catches up with the precursor shock. We note that these results show qualitatively similar features to the simulation results in [15, figure 10],
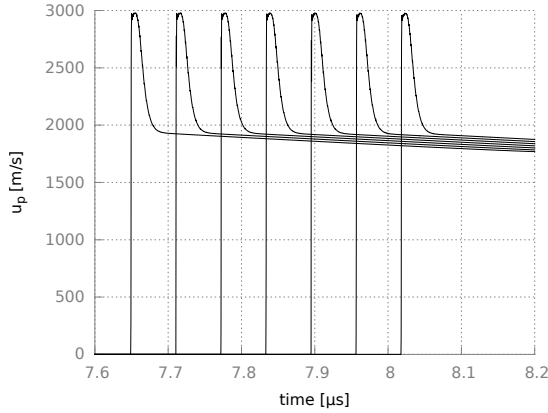
Figure 5: Steady travelling detonation wave recorded at gauges between 48 mm and 50 mm away from point of ignition.

Figure 7: Shock induced ignition of liquid nitromethane with input pressure of 9.2 GPa. Profiles of pressure and mass fraction are shown at intervals of 0.1 μs after the initial impact.
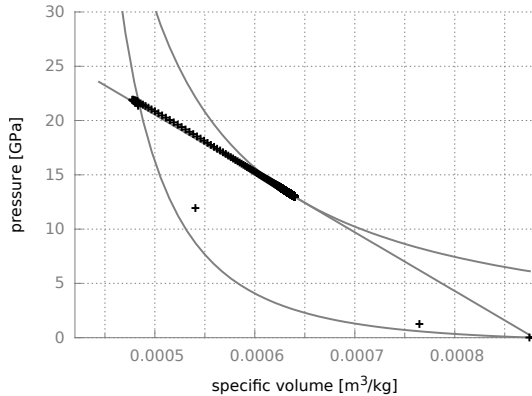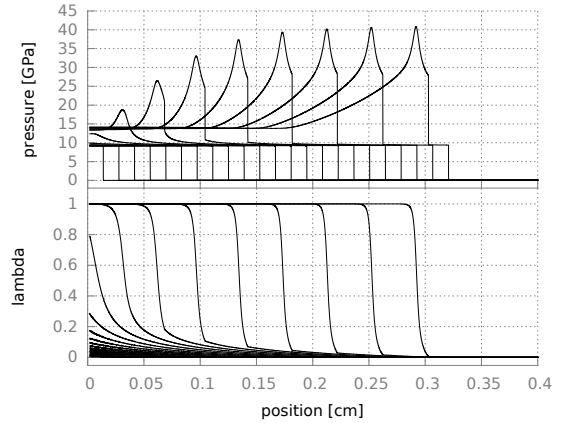

Figure 6: Simulation results for a steady travelling detonation wave, captured 10 μs after ignition. The simulation data (points) are overlaid on the Hugoniot curves from figure 2, demonstrating that the detonation wave is in CJ state.

including the structure of the leading wave just before it overtakes the precursor shock.

To compare with the experimental results in [21, figure 5], we simulate embedded velocity gauges. The first (stirrup) gauge at the interface with the impactor is not included as the simulation does not model this part of the experiment, but the placement of the other eight gauges matches the experimental setup. The velocity of the fluid impacting the boundary is chosen such that the input shock pressure of 9.2 GPa is the same as in the experiment. Results are shown in figure 8 and reasonable qualitative agreement with [21, figure 5] is apparent.

The timescale of the ignition and formation of the detonation wave is very similar to the experiment, with the first pressure pulse at ~ 0.8 μs and the overtake at ~ 1.2 μs in both the experimental and simulation results. Furthermore, if we take into account the limited temporal resolution of the experimental results and disregard the narrow spikes at the top of the reaction wave not captured by the experimental measurement, the peak velocity of the wave is close
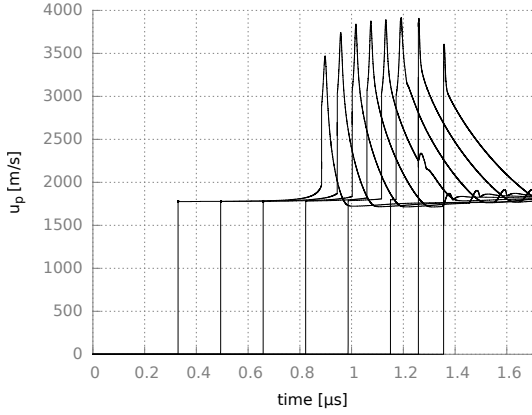
7

Figure 8: Shock ignition simulation as described in figure 7. Velocity histories are shown from eight simulated gauges placed to match the experimental setup in [21, figure 5]. The gauges are placed from 1.5 mm to 6.75 mm, separated by 750 μm.
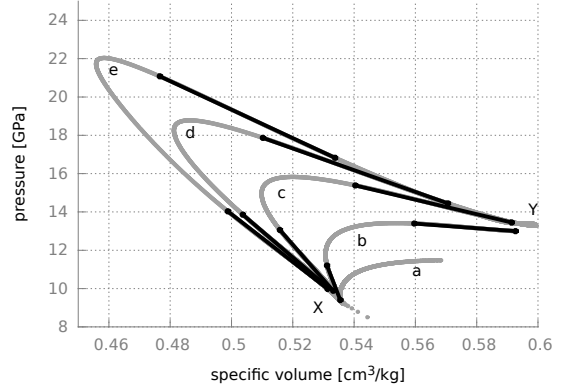

Figure 9: Early stages of the shock initiation process, simulated as described in figure 7, shown at times 0.74 μs, 0.76 μs, 0.78 μs, 0.80 μs and 0.82 μs. Labels a-e correspond to times on figure 11.

to the experimental value of $3\,\mathrm{km\,s^{-1}}$.

To analyse the results, the data for pressure versus position and specific volume versus position are plotted against each other to show the evolution on the (p,v) plane. A Hough transform-based analysis method is applied to identify the straight Rayleigh line structures. In figures 9 and 10 the output from the numerical simulation is shown as points and the identified Rayleigh lines are overlaid as solid lines. Figure 9 shows the first stages of the ignition at times 0.74 μs, 0.76 μs, 0.78 μs, 0.80 μs and 0.82 μs, before the emergence of a second shock wave. Figure 10 shows the later stages of the evolution at 0.84 μs and 0.92 μs where the reaction wave is approaching the precursor shock.

In these plots, flow starts at point 'X', in the state downstream of the precursor shock and upstream of the reaction wave. The final state, where the fluid meets the reflective boundary, is at the right hand edge of the diagram at point 'Y'.

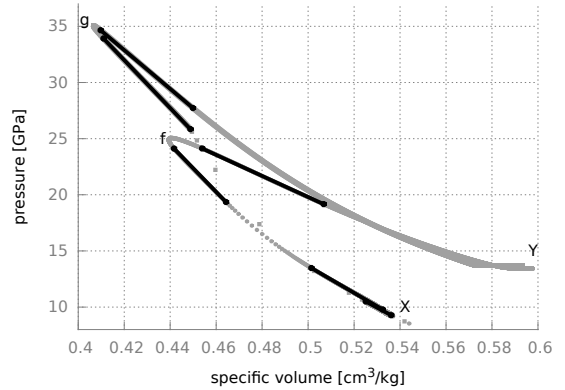In the early stages of the ignition, shown in fig-

Figure 10: Late stages of the shock initiation process, as described in figure 9, shown at times 0.84 μs and 0.92 μs. The shock that forms inside the reaction wave packet can be seen as the string of widely spaced points. Labels f-h correspond to times on figure 11.

8

ure 9, we observe sets of straight lines of negative slope on the compression (increasing p and deceasing v) and the expansion (decreasing p and increasing v) sides of the curves. Following the arguments in Singh and Clarke [22] and observing that the Mach numbers are supersonic throughout the former and subsonic at the latter, these can be identified as quasi-steady weak detonations and fast flames. The weak detonation does not consume all of the fuel and so the reaction continues in an unsteady region before the emergence of the fast flame and eventually an inert expansion (Taylor-like) wave.

At the later times shown in figure 10, the results indicate that a second weak detonation emerges near the head of the reaction wave. The flow between the two weak detonations steepens to form an internal shock wave and this quasi-steady group of four waves continues to move through the material.

This is markedly different from what is observed in gaseous ignition (see [1] and [17]), where the reaction wave behind the precursor shock evolves to form a steady detonation wave. In this case we see that the condensed material does not fully detonate behind the precursor shock but instead forms a compound wave similar to the "triplet" described in [22], composed of two weak detonations separated by an internal shock, and a fast flame.

This compound wave propagates as a coherent wave packet, as indicated by the (x, t) plot shown in figure 11. The path of the weak detonations, the fast flame and the reaction shock wave are shown. The precursor shock is located to the right of the region shown in the plot. The fast flame forms first, growing from a point close to the reflective boundary. Both waves move into the bulk of the material, where the second weak detonation and reaction shock emerge, as described above.

Conclusions

The shock-induced ignition of the condensed-phase explosive nitromethane was simulated with a reflected precursor shock wave travelling through the
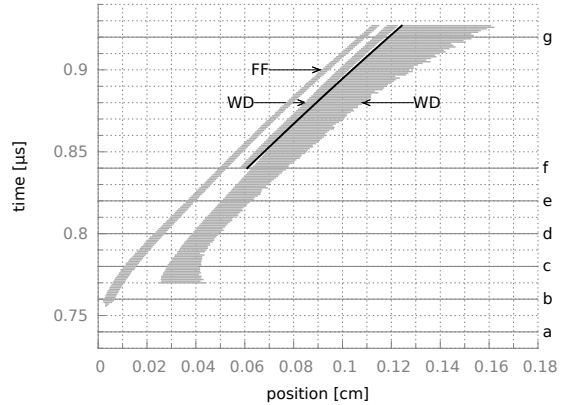

Figure 11: Location of the reaction waves during ignition. The regions of weak detonations are marked WD, the regions of fast flame marked FF and the shock that forms is shown with the solid line. The times marked a-g correspond to the curves in figures 9 and 10.

explosive. Using a Hough transform-based analysis technique we were able to identify, locate and characterise transient, quasi-steady waves in the unsteady flow between the times when the reaction wave emerges and when it overtakes the precursor shock. These quasi-steady phenomena are similar to those observed in the gaseous case, albeit in a more complex combination.

The results presented here are based on initial investigations. To confirm that these results do indeed reflect the physical behaviour of the material, it will be necessary to closely examine the assumptions in the mathematical model. In particular, the authors intend to repeat this analysis with simulation results from a model that does not depend on the temperature equilibrium closure condition, and also investigate other equations of state and reaction rates.

To explore the implications of these results, it will be important to analyse other ignition scenarios such as ignition by temperature gradients or hotspots. With

9

this understanding we plan to carry out similar analyses on other condensed phase explosives including the development of mesoscale models for shock initiation of heterogeneous explosives, such as PBXs.

Acknowledgements

References

[1] K. Bates. *Numerical simulation and analysis of the transition to detonation in gases*. PhD thesis, Cambridge University, 2005.

[2] J.B. Bdzil, R. Menikoff, S.F. Son, A.K. Kapila, and D. Scott Stewart. Two-phase modeling of deflagration-to-detonation transition in granular materials: A critical examination of modeling issues. *Physics of Fluids*, 1999.

[3] M. Braithwaite. private communication, 2014.

[4] W. Byers Brown, Z. Feng, and M. Braithwaite. Williamsburg equation of state for modelling non-ideal detonation. *Journal de Physique*, 1995.

[5] A. W. Campbell, W. C. Davis, and J. R. Travis. Shock initiation in liquid explosives. *Physics of Fluids*, 1961.

[6] J. F. Clarke. Fast flames, waves and detonation. *Progress in energy and combustion science*, 1989.

[7] C. A. Handley. Initial modelling of two HMX-based plastic bonded explosives at the mesoscale. In *Proceedings of the 14th International Detonation Symposium*, 2010.

[8] D. R. Hardesty. An investigation of the shock initiation of liquid nitromethane. *Combustion and Flame*, 1976.

[9] H. R. James and B. D. Lambourne. On the systematics of particle velocity histories in the shock-to-detonation transition regime. *Journal of Applied Physics*, 2006.

[10] A.K. Kapila, R. Menikoff, J.B. Bdzil, S.F. Son, and D. Scott Stewart. Two-phase modeling of deflagration-to-detonation transition in granular materials: Reduced equations. *Physics of Fluids*, 2001.

[11] B. Leal-Crouzet, G. Baudin, and H. N. Presles. Shock initiation of detonation in nitromethane. *Combustion and Flame*, 2000.

[12] P. C. Lysne and D. R. Hardesty. Fundamental equation of state of liquid nitromethane to 100 kbar. *Journal of Chemical Physics*, 1973.

[13] S. P. Marsh, editor. *LASL Shock Hugoniot Data*. University of California Press, 1980.

[14] R. Menikoff. On beyond the standard model for high explosives: Challenges & obstacles to surmount. In *Proceedings of the APS: Shock Compression of Condensed Matter*, 2009.

[15] R. Menikoff and M. S. Shaw. Modeling detonation waves in nitromethane. *Combustion and Flame*, 2011.

[16] L. Michael. *Numerical Simulations of Shock-Induced Void Collapse in Liquid Explosives*. PhD thesis, Cambridge University, 2012.

[17] N. Nikiforakis and J. F. Clarke. Quasi-steady structures in the two-dimensional initiation of detonations. *Proceedings of the Royal Society*, 1996.

[18] F. Petitpas, R. Saurel, E. Franquet, and A. Chinnayya. Modelling detonation waves in condensed energetic materials: multiphase CJ conditions and multidimensional computations. *Shock waves*, 2009.

[19] R. C. Ripley, F. Zhang, and F. S. Lien. Detonation interaction with metal particles in explosives. In *Proceedings of the 13th International Detonation Symposium*, 2006.

[20] G. J. Sharpe and M. Short. Shock-induced ignition of thermally sensitive explosives. *Journal of Applied Mathematics*, 2004.

[21] S. A. Sheffield, D. M. Dattelbaum, R. Engelke, R. R. Alcon, B. Crouzet, L. Robbins, D. B. Stahl, and R. L. Gustavsen. Homogeneous shock initiation process in neat and chemically sensitized nitromethane. In *Proceedings of the 13th International Detonation Symposium*, 2006.

[22] G. Singh and J. F. Clarke. Transient phenomena in the initiation of a mechanically driven plane detonation. *Proceedings of the Royal Society*, 1992.

[23] D. S. Stewart and S. Yoo. Equation of state for modeling the detonation reaction zone. *12th International Detonation Symposium*, 2002.

[24] C. M. Tarver and P. A. Urtiew. Theory and modeling of liquid explosive detonation. *Journal of Energetic Materials*, 2010.

[25] E. F. Toro. *Riemann solvers and numerical methods for fluid dynamics*. Springer, 2009.

[26] I. M. Voskoboinikov, V. M. Bogomolov, and A. Ya. Apin. Calculation of the initiation pressure of shock initiated homogeneous explosives. *Fizika Goreniya i Vzryva*, 1968.

[27] J. M. Winey, G. E. Duvall, M. D. Knudson, and Y. M. Gupta. Equation of state and temperature measurements for shocked nitromethane. *Journal of Chemical Physics*, 2000.